Letter of Intent to the Jefferson Lab Program Advisory Committee

Measuring the Charged Pion Polarizability in the $\gamma\gamma \to \pi^+\pi^-$ Reaction

R. Miskimen, A. Mushkarenkov
University of Massachusetts, Amherst, MA

D. Lawrence, E. Smith
Jefferson Laboratory, Newport News, VA

1 Abstract

This Letter of Intent presents our plan to make a new measurement of the charged pion polarizability $\alpha_\pi - \beta_\pi$ through measurements of $\gamma\gamma \to \pi^+\pi^-$ cross sections using the GlueX detector in Hall D. The charged pion polarizability ranks among the most important tests of low-energy QCD presently unresolved by experiment . Analogous to precision measurements of $\pi^0 \to \gamma\gamma$ testing the intrinsic odd-parity (anomalous) sector of QCD, the pion polarizability tests the intrinsic even-parity sector of QCD.

2 Introduction

Electromagnetic polarizabilities are fundamental properties of composite systems such as molecules, atoms, nuclei, and hadrons [Ho90]. Whereas magnetic moments provide information about the ground state properties of a system, polarizabilities provides information about the excited states of the system. For atomic systems the polarizabilities are of order the atomic volume. For hadrons the polarizabilities are much smaller than the volume, typically of order $10^{-4} fm^3$, because of the greater stiffness of the QCD force as compared to the electromagnetic force. Measurements of hadron polarizabilities provide an important test point for effective field theories, dispersion theories, and lattice calculations.

Hadron polarizabilities are best measured in Compton scattering experiments, where in the case of nucleon polarizabilities, one looks for a deviation of the cross section from the prediction of Compton scattering from a structureless Dirac particle. The electric and magnetic polarizabilities of the proton, α_p and β_p, have been measured in Compton scattering experiments at Mainz and other laboratories [Sc05], and in the near future it can be expected that neutron polarizabilities can be extracted from Compton scattering experiments on the deuteron and ^3He.

Because a free pion target doesnt exist, the measurements to date of the charged pion polarizability have been plagued by experimental and theoretical uncertainties. This letter of intent presents a plan to make a new measurement of the charged pion polarizability by measurement of $\gamma\gamma \to \pi^+\pi^-$ cross sections using the GlueX detector in Hall D.

3 Theoretical predictions for the charged pion polarizability

Theory for the the charged pion polarizability results directly from the original formulation of chiral perturbation theory (ChPT) by Gasser and Leutwyler [Ga84]. This lagrangian is invariant under the transformation $\phi_i \to -\phi_i$, where ϕ_i represents the eight Goldston boson fields, and has the feature that it doesn't allow transitions between even and odd numbers of mesons. For example, the transition $\pi^0 \to \gamma\gamma$ is not allowed at leading order $O(p^4)$ [Ho92]. For this reason the lagrangian must be augmented by the Wess-Zumino-Witten anomaly [We71]. Recently the PRIMEX experiment at JLab made a precision test of the intrinisic odd-parity (anomalous) sector of low-energy QCD by measuring the radiative width for $\pi^0 \to \gamma\gamma$ [Primex]. A measurement of the charged pion polarizability probes the intrinsic even-parity sector of QCD.

PCAC and leading order $O(p^4)$ chiral perturbation theory (ChPT) both predict that the electric and magnetic polarizabilities of the charged pion (α_π and β_π) are related to the charged pion weak form factors F_V and F_A in the decay $\pi^+ \to e^+\nu\gamma$

$$\alpha_\pi = -\beta_\pi \propto \frac{F_A}{F_V} = \frac{1}{6}(l_6 - l_5) \tag{1}$$

where l_5 and l_6 are low energy constants in the Gasser and Leutwyler effective Lagrangian [Ga84] Using recent results from the PIBETA collaboration for F_A and F_V [By09], the $O(p^4)$ ChPT prediction for the charged pion electric and magnetic polarizabilities is given by

$$\alpha_\pi = -\beta_\pi = 2.78 \pm 0.1^{-4} fm^3 \tag{2}$$

The $O(p^6)$ corrections are predicted to be relatively small [Bu96,Ga06], giving the following results,

$$\alpha_\pi - \beta_\pi = 5.7 \pm 1.0 \times 10^{-4} fm^3 \tag{3}$$

$$\alpha_\pi + \beta_\pi = 0.16 \pm 0.1 \times 10^{-4} fm^3 \tag{4}$$

Dispersion relations have also been used to find α_π and β_π, where $\gamma\gamma \to \pi^+\pi^-$ data are used to fix the dispersion integrals. Fitting $\gamma\gamma \to \pi^+\pi^-$ data from threshold up to 2.5 GeV, Fil'kov et. al. [Fi06] found that

$$\alpha_\pi - \beta_\pi = 13.0 + 2.6 - 1.9 \times 10^{-4} fm^3 \tag{5}$$

$$\alpha_\pi + \beta_\pi = 0.18 + 0.11 - 0.02 \times 10^{-4} fm^3 \tag{6}$$

which is in disagreement with ChPT.

Pasquini et al. [Pa08] examined the Fil'kov calculation in detail, and noted that the energy extrapolations used by Fil'kov below and above meson resonances leave considerable room for model dependence. When the basic requirements of dispersion relations are taken into account , Pasquini et al. found that dispersion relations predict

$$\alpha_\pi - \beta_\pi = 5.7 \times 10^{-4} fm^3 \tag{7}$$

which is in agreement with ChPT.

4 Pion polarizability and Standard Model corrections to $g_\mu - 2$

It is well known that there is a significant difference, 3.6σ , between the E821 experimental value for muon $g_\mu - 2$ and the standard mode (SM) prediction. The errors in $(g_\mu - 2)/2$ are approximately 63×10^{-11} for experiment , and 49×10^{-11} for theory. Since the next generation $g_\mu - 2$ experiment at FNAL will reduce the experimental error by a factor of four, it is very important to reduce the SM error by a similar factor. The two largest uncertainties in the SM prediction are from hadronic vacuum polarizaton and hadronic light-by-light (HLBL) scattering. In a recent preprint Ramsey-Musolf and collaborators report that an omitted contribution to HLBL from the pion polarizability is substantial and potentially significant [En12]. Work is continuing on this problem.

5 Measurements of the charged pion polarizability

Three different experimental techniques that have been utilized to measure α_π and β_π.

- Radiative pion photoproduction, $\gamma p \to \gamma' \pi^+ n$, at very low momentum transfer to the recoil nucleon. This reaction can be visualized as Compton scattering off a virtual pion. At forward Compton angles the reaction is sensitive to $\alpha_\pi + \beta_\pi$, and at backward angles $\alpha_\pi - \beta_\pi$. The most recent measurement has been from Mainz [Ah05] . Using the constraint $\alpha_\pi = -\beta_\pi$ they obtained

$$\alpha_\pi - \beta_\pi = 11.6 \pm 1.5_{stat} \pm 3.0_{sys} \pm 0.5_{model} \times 10^{-4} fm^3 \tag{8}$$

  Combining errors in quadature gives 3.4 in the standard units, which differs by 1.7σ from the ChPT prediction.

- Primakoff effect of scattering a high energy pion in the Coulomb field of a heavy nucleus, $\pi A \to \pi' \gamma A$. This reaction is equivalent to Compton scattering a nearly real photon off the pion. The most recent measurement has been from Serpukov [An83] . Using the constraint $\alpha_\pi = -\beta_\pi$, they obtained

$$\alpha_\pi - \beta_\pi = 13.6 \pm 2.8_{stat} \pm 2.4_{sys} \times 10^{-4} fm^3 \tag{9}$$

Combining errors in quadrature gives 3.7 in the standard units, differing by 2.1σ from the ChPT prediction. The COMPASS collaboration at CERN has also taken data, and analysis is underway.

- $\gamma\gamma \to \pi^+\pi^-$. By crossing symmetry (exchanging s and t variables in the scattering amplitude) the $\gamma\gamma \to \pi\pi$ amplitude can be related to the $\gamma\pi \to \gamma\pi$ amplitude. For the $\gamma\gamma \to \pi\pi$ reaction , the sensitivity to the polarizabilities goes as $\alpha_\pi - \beta_\pi$. Babusci et al. [Ba92] used chiral perturbation theory with a one-loop correction to derive a formula they used to obtain pion polarizabilites from $\gamma\gamma \to \pi^+\pi^-$ data. Examining data sets from PLUTO, DM1, DM2, and MARK II , they obtained values of $\alpha_\pi - \beta_\pi$ ranging from 52.6 ± 14.8 (from DM2) to 4.4 ± 3.2 (from MARK II).

It is difficult to draw conclusions from the present experimental results for $\alpha_\pi - \beta_\pi$. It is generally recognized that the most model independent technique to measure hadron polarizabilities is through Compton scattering. The two most recent Compton measurements at Serpukov (Primakov) and Mainz (virtual pion) agree that the value for $\alpha_\pi - \beta_\pi$ is approximately twice the size predicted by ChPT, albeit with large errors. The data are also in agreement with the dispersion calculation by Fil'kov. New data from Compass are especially welcome to help resolve the situation.

Turning now to the $\gamma\gamma \to \pi^+\pi^-$ data, the analysis by Babusci [Ba92] was limited by data sets with low statistics (MARK-II) and large systematic errors (see comments by Pennington in [Mo87]). It was also limited by the theoretical model, which was only one-loop in ChPT. Since then, considerable theoretical progress has been make in calculating $\gamma\gamma \to \pi\pi$ cross sections; (i) Gasser et al. [Ga06] performed a two-loop calculation in ChPT , (ii) Donoghue and Holstein [Do93] established a connection between dispersiion theory and ChPT by matching the low-energy chiral amplitude with the dispersion treatment, and (iii) Pasquini et al. [Pa08] performed a purely dispersiive treatment for the cross section.

Fig. 1 shows predicted total cross sections from Pasquini et al. for $\gamma\gamma \to \pi^+\pi^-$ for $|cos\theta_{\pi\pi}| < 0.6$. The red curve is the Born approximation calculation with no polarizability effect. The black solid curve is an unsubtracted dispersion relation (DR) calculation with $\alpha_\pi - \beta_\pi = 5.7$, and the dashed curve is the subtracted DR calculation with the same polarizability. The dotted curve is the subtracted DR calculation with the polarizabilities from [Fi06] with $\alpha_\pi - \beta_\pi = 13.0$. Comparision of the subtracted DR curves with $\alpha_\pi - \beta_\pi$ equal to 5.7 (dashed) and 13.0 (dotted), shows a change in the peak cross section at $W_{\pi\pi} \approx 0.3$ GeV by approximately 10 percent. We conclude that measurements of the pion polarizability through the $\gamma\gamma \to \pi^+\pi^-$ reaction will need statistical and systematic accuracies at the level of a few percent.

The experimental data in the figure are from MARK-II [Bo92], where there are probably less than 400 events in the region of interest, $W_{\pi\pi} < 0.5$ GeV. The figure clearly shows that the MARK-II data do not have the statistical precision, nor the coverage in $W_{\pi\pi}$, to provide a useful constraint on $\alpha_\pi - \beta_\pi$. It is useful to quote Donoghue and Holstein [Do93] here, " *We conclude that although $\gamma\gamma \to \pi^+\pi^-$ measurements certainly have the potential to provide a precise value for the pion polarizability, the statistical uncertainty of the present values does not allow a particularly precise evaluation.*"

6 Measurements of the charged pion polarizability at Jefferson Lab Hall D

We propose to make measurements of $\gamma\gamma \to \pi^+\pi^-$ cross sections via the Primakoff effect using the GlueX detector in Hall D. Starting from the Primakoff result for cross sections with incident *linearly polarized photons* [Gl61] and then generalizing for a two-body final state gives,

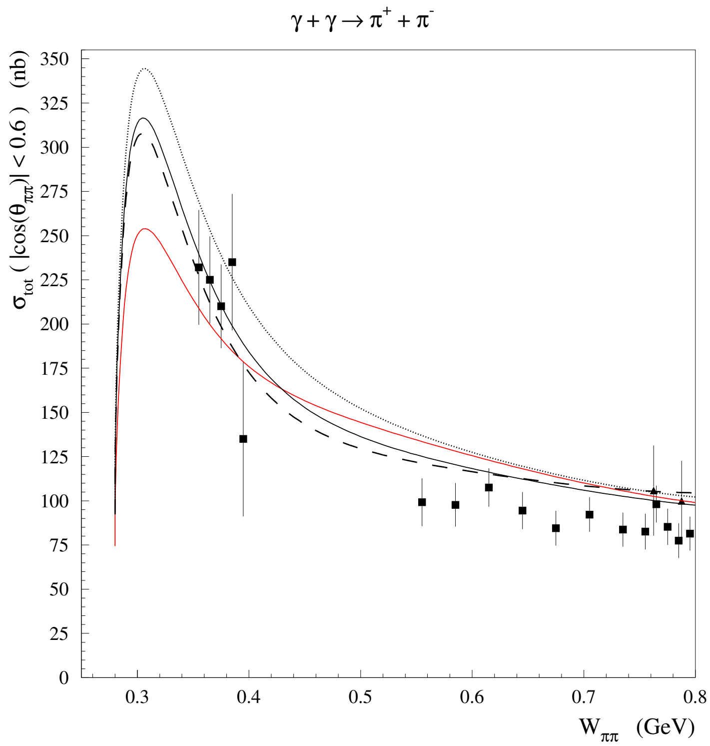

Figure 1: $\gamma\gamma \to \pi^+\pi^-$ cross sections. Red curve: Born approx. (no polarizability effect); black solid: unsubtracted DR calculation with $\alpha_\pi - \beta_\pi = 5.7$; dashed: subtracted DR with $\alpha_\pi - \beta_\pi = 5.7$; dotted: subtracted DR with $\alpha_\pi - \beta_\pi = 13.0$.

$$\frac{d^3\sigma}{d\Omega_{\pi\pi}^{Lab} d\Omega_\pi^{CM} dW_{\pi\pi}} = \frac{d^2\Gamma(\gamma\gamma \to \pi^+\pi^-)}{d\Omega_\pi^{CM} dW_{\pi\pi}} \frac{8\alpha Z^2}{W_{\pi\pi}^3} \frac{\beta^3 E_\gamma^4}{Q^4} |F_{EM}(Q)|^2 sin^2\theta_{\pi\pi}(1+P_\gamma cos2\phi_{\pi\pi}) \tag{10}$$

where the differential radiative width (rate) for $\gamma\gamma \to \pi^+\pi^-$ is given by

$$\frac{d^2\Gamma(\gamma\gamma \to \pi^+\pi^-)}{d\Omega_\pi^{CM} dW_{\pi\pi}} = \frac{d\sigma(\gamma\gamma \to \pi^+\pi^-)}{d\Omega_\pi^{CM}} \frac{W_{\pi\pi} k_\pi^{CM}}{8\pi^2} \tag{11}$$

In these expressions, $\Omega_{\pi\pi}^{Lab}$ is the lab solid angle for the emission of the $\pi\pi$ system, Ω_π^{CM} is solid angle for the emission of the π^+ in the $\pi\pi$ CM frame,

$W_{\pi\pi}$ is the $\pi\pi$ invariant mass, Z is the atomic number of the target, β is the velocity of the $\pi\pi$ system, E_γ is the energy of the incident photon, $F_{EM}(Q)$ is the electromagnetic form factor for the target with FSI corrections applied, $\theta_{\pi\pi}$ is the lab angle for the $\pi\pi$ system, $\phi_{\pi\pi}$ is the azimuthal angle relative to the incident photon polarizatoin, and k_π^{CM} is the momentum of the π^+ in the CM frame. Assuming a 5 percent radiation length lead target, tagged 8.5 GeV photons at a rate of 10^7 photons/s, and a running time of 500 hours, *then approximately 36,000 $\pi^+\pi^-$ Primakov events are produced in the near threshold region up to $W_{\pi\pi} = 0.5$ GeV.*

The largest physics background is from coherent ρ^0 photo-production on the nuclear target. In the helicity frame (described in Fig. 2) the angular distribution of the pions is given by [Ba72]

$$\frac{dW}{dcos\theta d\phi} = \frac{3}{8\pi} sin^2\theta_\pi (1 + P_\gamma cos2\Psi) \tag{12}$$

where Ψ is the azimuthal angle in the helicity frame relative to the photon polariation. The differential cross section for ρ^0 photo-production on nuclear targets is given by,

$$\frac{d\sigma}{dt} = \sigma(0)e^{At} \tag{13}$$

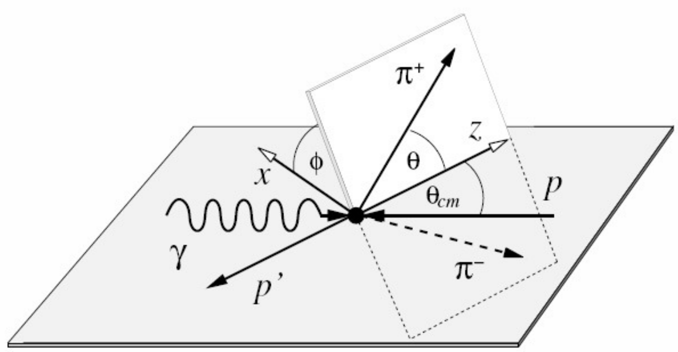

Figure 2: Diagram of the helicity frame for two pion photo-production on the nucleon

Other physics backgrounds result from nuclear coherent production of $\pi^+\pi^-$, and the nuclear incoherent production. It can be expected that the nuclear coherent production will be small compared to coherent ρ^0 production for two reasons. First, a nuclear target, specifically lead, acts as a filter to remove nuclear coherent events. This effect is clearly seen in the π^0 angular distributions measured by the PRIMEX experiment for carbon and lead [Primex], and the effect will be even stronger for the $\pi\pi$ final state. Because Primakoff production occurs approximtely 100 fm from the nucleus, FSI has a relatively weak effect on the Primakoff process even for heavy nuclei [Mi11]. Secondly, there should be little strength for 0^+ $\pi\pi$ production in the near threshold region resulting from $\gamma N \to f_0(600)N$. An analysis of $\pi\pi$ photoproduction using linearly polarized photons does not see evidence for this background [Ba72].

Nuclear incoherent production can result from final state interactions of coherently produced ρ^0 mesons with the nucleus. We are collaboratiing with T. Rodrigues, who did the nuclear incoherent calculations for PRIMEX, on a similar calculation for this experiment [Ro].

Histograms of Primakoff and coherent ρ^0 photo-production production with the event weighting given by Eqns. 10, 11, 12 , and 13 are shown in Figs. 3, 4, 5, 6, 7, and 8 . The $W_{\pi\pi}$ distribution for ρ^0 events is taken from a Zeus analysis of high-t ρ^0 photo-production on the proton [Br99]. The parameters $\sigma(0)$ and A in Eqn. 13 are taken from references [Al70] and [As67], respectively.

Fig. 3 shows the 2π invariant mass distribution for Primakoff and ρ^0 events up to a cutoff at $W_{\pi\pi} = 0.40$ GeV. The colors in the figure reference different regions in $W_{\pi\pi}$, blue is for events with $0.28 < W_{\pi\pi} < 0.32$ GeV, green is for events with $0.32 < W_{\pi\pi} < 0.36$ GeV, and red is for events with $0.36 < W_{\pi\pi} < 0.40$ GeV. In the blue region the Primakoff process dominates; in the red region ρ^0 photo-production dominates; and in the green region the Primakoff and VMD strengths are approximately equal. Fig. 4 shows how the strength of the Primakoff process depends on $W_{\pi\pi}$. The kinematic values shown in figures 5-8 illustrate their dependance on $W_{\pi\pi}$ using this same color scheme.

Fig. 5 shows the t distribution of events. The blue curve (primarily Primakoff) shows the characheristic peaking of the Primakoff process at very

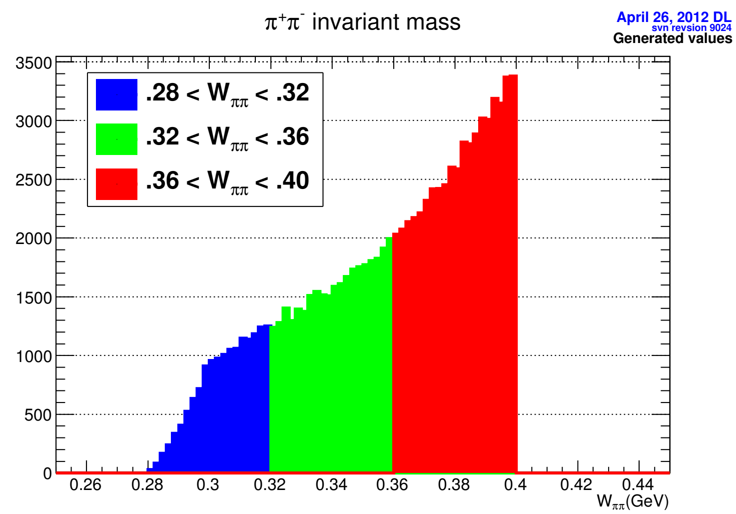

Figure 3: Histogram of $W_{\pi\pi}$ for Primakoff and ρ^0 events

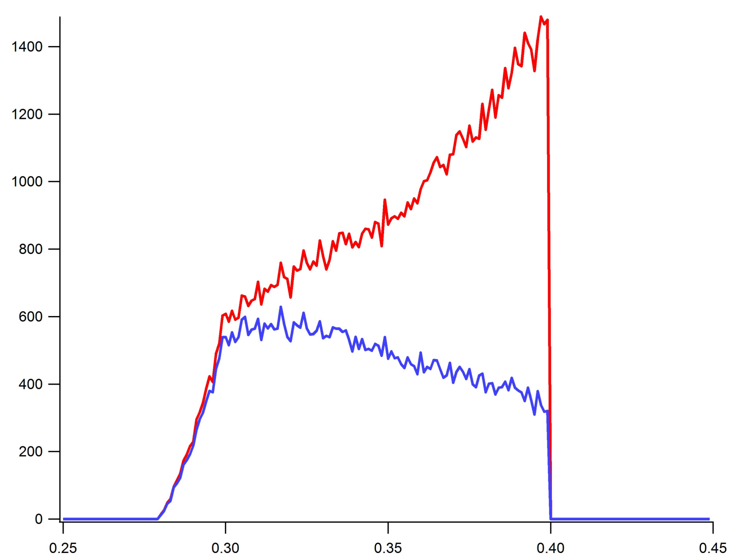

Figure 4: Histogram of $W_{\pi\pi}$ for Primakoff (blue curve) and Primakoff + ρ^0 events (red curve) events

low angles [Mi11]. The red curve (primarily ρ^0) is much flatter at low t , as expected by Eqn. 13.

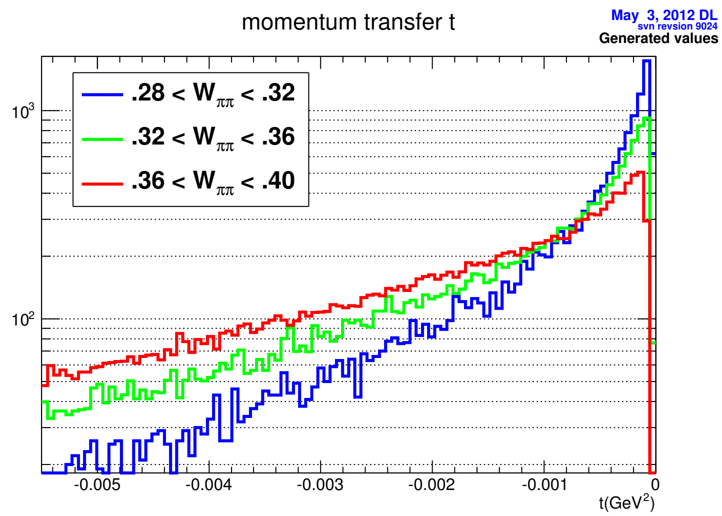

Figure 5: Histogram of t for Primakoff and ρ^0 events. The blue curve is for events with $0.28 < W_{\pi\pi} < 0.32$ GeV, green is for events with $0.32 < W_{\pi\pi} < 0.36$ GeV, and red is for events with $0.36 < W_{\pi\pi} < 0.40$ GeV.

Fig. 6 shows the distribution of azimuthal angles of the $\pi\pi$ system in the lab frame, where the angle $\phi_{\pi\pi}$ is measured relative to the incident photon polarizaton direction. The blue curve (primarily Primakoff) shows a prominent $(1 - cos2\phi_{\pi\pi})$ characteristic from Eqn. 10, and the red curve (primarily ρ^0) is nearly flat.

Fig. 7 shows the distribution of $\cos\theta_{\pi+}$ in the helicity frame. The blue curve (primarily Primakoff) is nearly flat because the threshold Primakoff pions are in s-waves . The red curve (primarily ρ^0) shows the $\sin^2\theta_\pi$ peaking from Eqn. 12 .

Fig. 8 shows the distribution of azimuthal angles of the π^+ in the helicity frame, where the angle ψ is measured relative to the incident photon polarizaton direction. The blue curve (primarily Primakoff) is nearly flat. The red curve (primarily ρ^0) shows a prominent $(1 - cos2\psi)$ characteristic from Eqn. 12.

Based on the sensitivity of the reaction process to incident linearly polarized photons demonstrated in these figures, we estimate that it will be possible to separate contributions from the Primakoff process from coherent

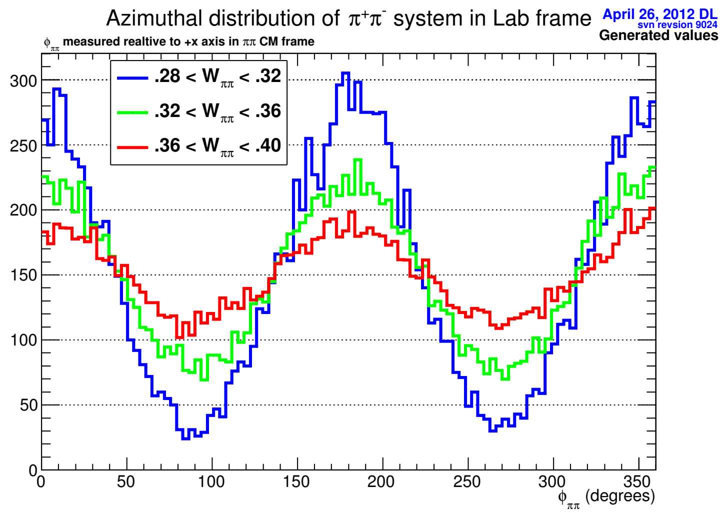

Figure 6: Histogram of $\phi_{\pi\pi}$ for Primakoff and ρ^0 events . The blue curve is for events with $0.28 < W_{\pi\pi} < 0.32$ GeV, green is for events with $0.32 < W_{\pi\pi} < 0.36$ GeV, and red is for events with $0.36 < W_{\pi\pi} < 0.40$ GeV.

ρ^0 photoproduction by measuring (i) the t distribution of the pion pairs, (ii) the azimuthal distribution of the $\pi\pi$ system in the lab frame relative to the photon polarization ($\phi_{\pi\pi}$) , and (iii) the azimuthal distribution of π^+ in the helicity frame relative to the photon polarization (ψ) . Plans for the Hall D photon source call for a peak in the coherent bremstrahlung at an energy of 8.5 to 9.0 GeV, with a photon polarization of approximately 40 percent.

7 Simulation

The simulation effort to support this measurement is just beginning. The standard GlueX simulation and reconstruction software $sim-recon$ is being used. The simulation is done using GEANT3 and has a detailed description of the geometry (fig. 9 shows a diagram of the GlueX detector). Hits generated by the simulation are smeared using known detector resolutions. Full reconstruction is done using only the hits. This includes track finding and track fitting using a Kalman filter tracking program developed for GlueX. Fig. 10 shows a histogram of θ_{π^+} for reconstructed π^+ tracks that start

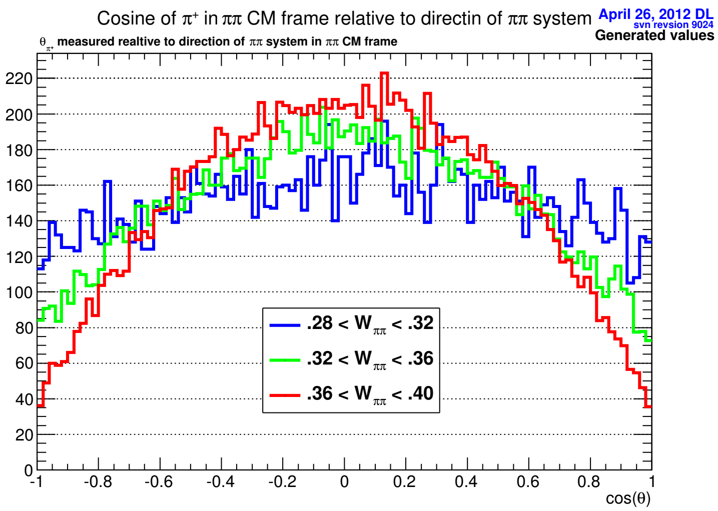

Figure 7: Histogram of $\cos\theta_{\pi^+}$ in the helicity frame for Primakoff and ρ^0 events . The blue curve is for events with $0.28 < W_{\pi\pi} < 0.32$ GeV, green is for events with $0.32 < W_{\pi\pi} < 0.36$ GeV, and red is for events with $0.36 < W_{\pi\pi} < 0.40$ GeV.

at the standard target position. For the purposes of this study, the 30cm LH_2 GlueX target was replaced with a 5% rad. len. Pb target to better represent the conditions being considered for this measurement. The single track acceptance above 1^o, the approximate low angle cutoff for the FDC's, is approximately 50 % from this very preliminary study. To optimize the acceptance for low mass pion pairs, we are considering moving the target 1 m upstream from the nominal target position. This should improve the acceptance for very forward going pions to reach the forward drift chambers (FDC) in GlueX.

Future work planned in the development of a proposal includes:

- Calculation of acceptance and resolutions in $W_{\pi\pi}$, t , $\phi_{\pi\pi}$, $\cos\theta_\pi$ and ψ
- Optimizing the acceptance and resolution with respect to the target position
- Event simulation with electromagnetic and hadronic backgrounds

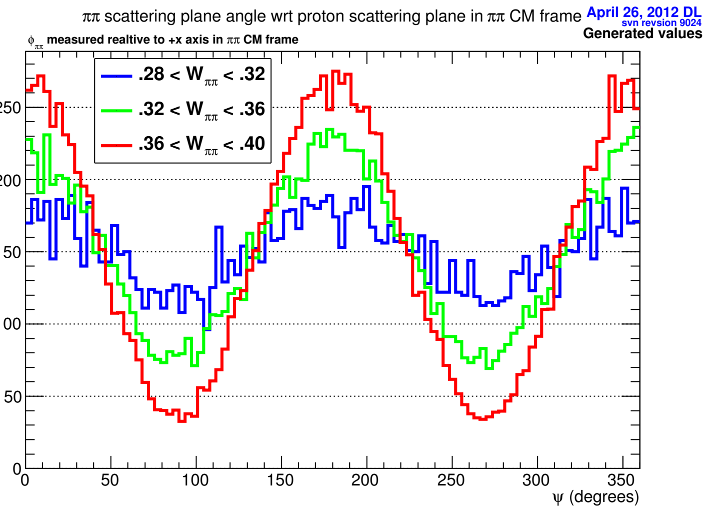

Figure 8: Histogram of ψ for Primakoff and ρ^0 events . The blue curve is for events with $0.28 < W_{\pi\pi} < 0.32$ GeV, green is for events with $0.32 < W_{\pi\pi} < 0.36$ GeV, and red is for events with $0.36 < W_{\pi\pi} < 0.40$ GeV.

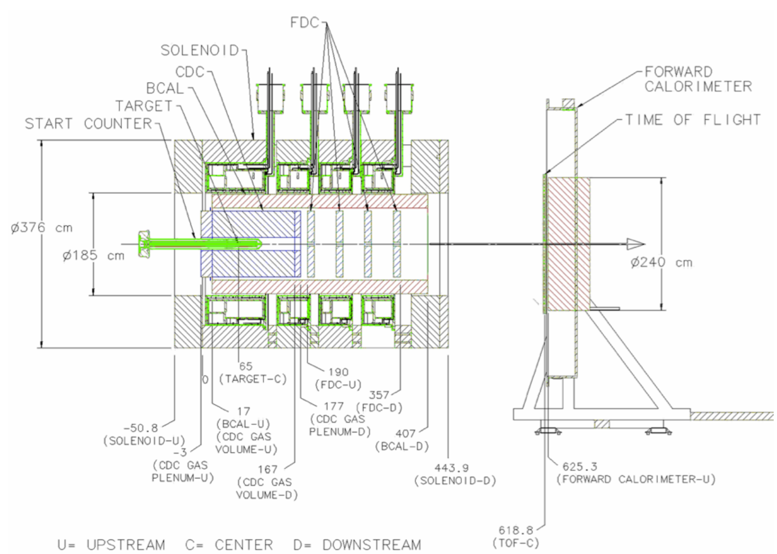

Figure 9: Diagram of the GlueX detector

- Optimizing the incident photon energy, degree of linear polarization, and photon rate for this measurement

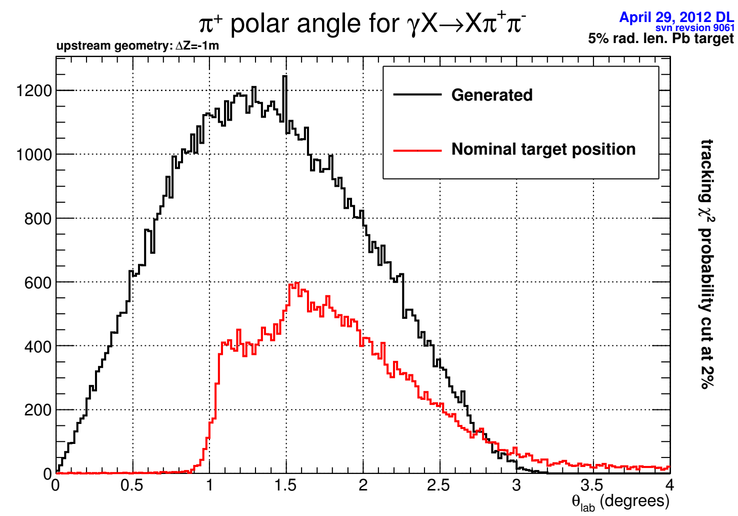

Figure 10: Histogram of θ_{π^+} for accepted π^+ tracks

- Estimate for the experimental uncertainty in measuring $\alpha_\pi - \beta_\pi$

References

[Ah05] J. Ahrens et al., Eur. Phys. J. A23, 113 (2005).
[Al70] H. Alvensleben et al., Phys. Rev. Lett. 24, 786 (1970).
[An83] Yu. M. Antipov et al., Phys. Lett. B121, 445 (1983).
[As67] J. Asbury et al., Phys. Rev. Lett. 19, 865 (1967)
[Ba72] J. Ballam, et al., Phys Rev D 5, 545 (1972).
[Ba92] D. Babusci, et al. Phys. Lett. B 277, 158 (1992).
[Bo92] J. Boyer et al. (MARK-II collaboration), Phys. rev. D 42, 1350 (1990).
[Br99] J. Bretweg et al., arxiv:hep-ex/9910038v1 (1999).
[Bu96] U. Burgi, Nucl. Phys. B479, 392 (1996)
[By09] M. Bychkov et al., Phys. Rev. Lett., 103, 051802 (2009).
[Do93] J. F. Donoghue and B. R. Holstein, Phys. Rev. D 48, 137 (1993).
[En12] K. Engel, H. Patel, M. Ramsey-Musolf, arXiv:1201.0809v2 [hep-ph]
[Fi06] L.V. Fil'kov and V.L. Kashevarov, Phys. Rev. C 73, 035210 (2006).
[Ga84] J. Gasser and H. Leutwyler, Ann. Phys. 158, 142 (1984).
[Ga06] J. Gasser, M.A. Ivanov, and M. E. Sainio, Nucl. Phys. B745, 84 (2006).
[Gl61] V. Glaser, and R. A. Ferrell, Phys. Rev. 121, 886 (1961).
[Ho90] B. Holstein, Comm. Nucl. Part. Phys. 19, 221 (1990)
[Ho92] B. Holstein, Nucl. Phys. A546, 213 (1992).
[Mi11] R. Miskimen,
[Mo87] D. Morgan and M.R. Pennington, Phys. Lett. B 192 (1987).
[Pa08] B. Pasquini, D. Drechsel, and S. Scherer, Phys. Rev. C 77, 06521 (2008).
[Primex]
[Ro] T. Rodrigues, private communication
[Sc05] M. Schumacher, Prog. Part. and Nucl. Phys. 55, 567 (2005).
[We71] J. Wess and B. Zumino, Phys. Lett. 37B, 422 (1971), and E. Witten, Nucl. Phys. B223, 422 (1983).